Journal of Molecular and Cellular Cardiology 134 (2019) 144–153

Contents lists available at ScienceDirect

Journal of Molecular and Cellular Cardiology

journal homepage: www.elsevier.com/locate/yjmcc

Remodeling of substrate consumption in the murine sTAC model of heart failure

Aslan Turer[a], Francisco Altamirano[a], Gabriele G. Schiattarella[a], Herman May[a], Thomas G. Gillette[a], Craig R. Malloy[b,c,d], Matthew E. Merritt[e,*]

[a] Department of Internal Medicine, UT Southwestern Medical Center, Dallas, TX 75390, United States of America
[b] Advanced Imaging Research Center, UT Southwestern Medical Center, Dallas, TX 75390, United States of America
[c] Department of Radiology, UT Southwestern Medical Center, Dallas, TX 75390, United States of America
[d] VA North Texas Healthcare System, Lancaster, TX, United States of America
[e] Department of Biochemistry and Molecular Biology, University of Florida, Gainesville, FL 32610-0245, United States of America

ARTICLE INFO

Keywords:
Substrate selection
Glucose
Ketones
Fatty acids
Anaplerosis

ABSTRACT

Background: Energy metabolism and substrate selection are key aspects of correct myocardial mechanical function. Myocardial preference for oxidizable substrates changes in both hypertrophy and in overt failure. Previous work has shown that glucose oxidation is upregulated in overpressure hypertrophy, but its fate in overt failure is less clear. Anaplerotic flux of pyruvate into the tricarboxylic acid cycle (TCA) has been posited as a secondary fate of glycolysis, aside from pyruvate oxidation or lactate production.

Methods and results: A model of heart failure that emulates both valvular and hypertensive heart disease, the severe transaortic constriction (sTAC) mouse, was assayed for changes in substrate preference using metabolomic and carbon-13 flux measurements. Quantitative measures of O_2 consumption in the Langendorff perfused mouse heart were paired with ^{13}C isotopomer analysis to assess TCA cycle turnover. Since the heart accommodates oxidation of all physiological energy sources, the utilization of carbohydrates, fatty acids, and ketones were measured simultaneously using a triple-tracer NMR method. The fractional contribution of glucose to acetyl-CoA production was upregulated in heart failure, while other sources were not significantly different. A model that includes both pyruvate carboxylation and anaplerosis through succinyl-CoA produced superior fits to the data compared to a model using only pyruvate carboxylation. In the sTAC heart, anaplerosis through succinyl-CoA is elevated, while pyruvate carboxylation was not. Metabolomic data showed depleted TCA cycle intermediate pool sizes versus the control, in agreement with previous results.

Conclusion: In the sTAC heart failure model, the glucose contribution to acetyl-CoA production was significantly higher, with compensatory changes in fatty acid and ketone oxidation not reaching a significant level. Anaplerosis through succinyl-CoA is also upregulated, and is likely used to preserve TCA cycle intermediate pool sizes. The triple tracer method used here is new, and can be used to assess sources of acetyl-CoA production in any oxidative tissue.

1. Introduction

From 2009 to 2014, the number of adults living with heart failure (HF) in the US increased from 5.7 million to 6.5 million, and cardiovascular disease remains the leading cause of death [1]. HF associated with valvular defects or hypertension commonly manifests at early stages as myocardial hypertrophy, which is metabolically distinct from hypertrophy associated with diabetic cardiomyopathy [2]. While metabolic changes associated with heart failure have long been known [3], the advent of ^{31}P NMR of the functioning myocardium enabled in situ determination of ATP kinetics and energy availability [4,5]. The noninvasive nature of magnetic resonance made it possible to measure ATP content and turnover in humans, where earlier measurements of decreasing ATP availability in preclinical models were largely confirmed [6]. These observations became a central pillar in a multifactorial model of HF that posits the heart is “an engine out of fuel”. In

* Corresponding author.
E-mail addresses: Aslan.Turer@UTSouthwestern.edu (A. Turer), Francisco.Altamirano@utsouthwestern.edu (F. Altamirano), Gabriele.Schiattarella@utsouthwestern.edu (G.G. Schiattarella), Herman.May@utsouthwestern.edu (H. May), thomas.gillette@utsouthwestern.edu (T.G. Gillette), craig.malloy@utsouthwestern.edu (C.R. Malloy), matthewmerritt@ufl.edu (M.E. Merritt).

https://doi.org/10.1016/j.yjmcc.2019.07.007
Received 3 October 2018; Received in revised form 1 July 2019; Accepted 17 July 2019
Available online 21 July 2019
0022-2828/

this model, the underlying etiology of mechanical failure is due to ATP shortage in the myocardium [7,8]. As such, metabolic modulation of energy production in the heart is a logical target for intervention [9].

Most energy production in the heart is derived from oxidation of fatty acids (FAs) [10]. Cardiac hypertrophy is metabolically identified by upregulated glucose oxidation or glycolytic flux [11,12]. These changes in fuel selection are driven by a reprogramming of gene expression in the failing heart to match that of the fetal heart [13]. This model places great emphasis on the efficiency of glucose for ATP production/per mol of O_2 consumption as compared to fatty acids or ketones [14]. Many studies have reported that glucose consumption is indeed upregulated in hypertrophy, although its ultimate fate is debated [15], as pyruvate derived from glucose can be oxidized via acetyl-CoA or serve as an anaplerotic substrate for replenishing TCA cycle intermediates. Alternatively, glucose can traverse the pentose phosphate pathway, or be shunted into the hexosamine biosynthetic pathway [16]. Recently, the view of increased glucose utilization as a protective adaptation of the heart has been called into question [17]. New experiments designed to increase fatty acid oxidation (FAO) in a pressure overloaded hypertrophy model demonstrate both metabolic and functional benefits to maintaining the normal profile of substrate selection [18]. A large literature exists using a 1–4 week pressure overload hypertrophy model produced by transaortic constriction (TAC) [19–21]. Constriction in this model is usually accomplished with a 27 gauge needle with initial compensated hypertrophy that progresses to decompensated hypertrophy and heart failure after 6 to 8 weeks [18,22,23]. A recent report described a different paradigm where TAC surgery is performed to induce hypertrophy followed by ligation of the left anterior descending coronary artery to induce a myocardial infarct and overt HF [24]. This study used metabolomic and flux measures to strongly suggest increased ketone oxidation in their model of HF. Findings in a TAC induced HF model without infarction showed increased β-hydroxybutyrate availability improved myocardial energy production by 18%, but without a concurrent gain in cardiac efficiency [25]. A recent study in BDH1 knockout mice using the TAC/infarction model and in dogs with pacing-induced HF posited that increased ketone oxidation is adaptive, being used as a metabolic stress defense [26]. Evidence of upregulated ketone oxidation in HF was also identified in a similar metabolomic study of humans [27]. Here we used an adaption of the TAC model called severe TAC (sTAC). In this model surgery is performed using a narrower 28 gauge needle, which produces an exaggerated hypertrophic response that devolves within a week to decompensated hypertrophy, quickly progressing to severe HF [28]. Perfused hearts from the sTAC murine model with clear HF, were studied in the presence of insulin using a triple-tracer approach paired with carbon-13 NMR that allows simultaneous assessment of substrate competition between glucose, FAs, and ketones in a single heart. It should be noted that the role of insulin in cardiac energetics in hypertrophy and failure remains essential [29]. The fractional contribution of exogenous carbohydrate versus non-carbohydrate sources to acetyl-CoA production is significantly different, while the contribution of endogenous sources (i.e., glycogenolysis, lipolysis) is unchanged. Unlike in previous experiments, we have detected increased anaplerotic flux via either succinyl-CoA or through glutamine/glutamate. Anaplerosis is the “refilling” of the TCA cycle intermediates that would be depleted by biosynthetic pathways that would otherwise consume them as substrates. Complementary metabolomic analysis shows depleted pools of TCA cycle intermediates in HF, in agreement with previous results in part [24], though in this model succinate is decreased. Anaplerosis of glutamine is thought to be limited in the heart [30]. Previously, pyruvate anaplerosis was demonstrated to be an essential part of heart function, supplying the oxaloacetate necessary for condensation with acetyl-CoA, producing citrate and allowing continued TCA cycle turnover [31]. If anaplerosis through succinyl-CoA is activated in HF as suggested here, it represents an alternative to ATP wasting pyruvate carboxylation [15] and a possible adaptive process that should be seen as beneficial in the failing heart.

2. Materials and methods

2.1. Materials

[1,6-$^{13}C_2$]glucose and [1,3-$^{13}C_2$]ethylacetoacetate were purchased from Sigma-Aldrich Isotec, Inc. (Miamisburg, OH). An algal mixture of uniformly ^{13}C enriched fatty acids (99%) was purchased from Cambridge Isotope Laboratories, Inc. (Tewksbury, MA). The ethylacetoacetate was hydrolyzed to acetoacetate immediately prior to use. All other compounds were used without further purification.

2.2. Aortic constriction

Aortic constriction surgery was approved by Institutional Animal Care and Use Committee of UT Southwestern Medical Center. The surgical method has been previously described [28]. Male C57BL/6 J mice, 14–16 weeks in age, were purchased from the UTSW mouse core and housed 4 to a cage. Briefly, animals were anesthetized using ketamine (100 mg/kg IP) plus xylazine (5 mg/kg IP), intubated, and ventilated at a rate of 120 breaths per minute and at a tidal volume of 0.1 mL. The aortic arch was accessed via a left lateral thoracotomy. Suture material (5–0 silk) was used to ligate the aorta (between the innominate and left carotid arteries) overlying a 28G needle to produce the sTAC model. The TAC mice were produced using a 27 gauge needle. After ligation, the needle was removed leaving a discrete region of stenosis in the aorta. The chest was closed and the animals were allowed to recover from anesthesia. Echocardiographic recordings reveal progressive deterioration of LV systolic function. In this model the aortic constriction leads to pressure-overload failure by three weeks [28]. Echocardiographic recordings were done prior to subsequent studies to confirm deterioration of LV systolic function. Only sTAC mice were used for the metabolomic and ^{13}C isotopomer analysis.

2.3. Perfusion protocol

The protocol was approved by the Institutional Animal Care and Use Committee of UT Southwestern Medical Center. All animals were fed ad libitum. A single ketamine (43 mg/kg) and xylazine (8.7 mg/kg) intraperitoneal injection was used for general anesthesia. Depth of anesthesia was assessed by observing the respiratory rate, paw pinch reflex, and palpebral reflex of the animal. Under general anesthesia, the hearts were rapidly excised and arrested in ice cold perfusion medium. Langendorff perfusions were performed according to Stowe, et al. [32], including measurements of developed pressure, coronary flow, heart rate, and O_2 consumption. O_2 consumptions were collected at 0, 15, 30, 45, and 60 min. The average of these numbers was used as the O_2 consumption for normalization of the ^{13}C isotopomer data. For the ^{13}C NMR analysis, a total of $N = 8$ hearts received the sham surgery, while $N = 7$ hearts were used for sTAC. Briefly, the aorta of the excised heart was cannulated and perfused in non-recirculating mode at a constant perfusion pressure of 80 cm H_2O. Hearts were perfused unloaded for a total of 60 min. A Krebs-Henseleit buffered medium containing 25 mM $NaHCO_3$, 118 mM NaCl, 4.7 mM KCl, 1.2 mM $MgSO_4$, 1.2 mM KH_2PO_4, and 0.5 mM ethylene diamine tetraacetic acid was continuously circulated through a thin film oxygenator with 95/5 mixture of O_2/CO_2 gas to maintain a pH of 7.4. The perfusing medium was maintained at 37 °C using a water bath. A pressure transducer was used to measure the heart rate. Typical heart rates were 200 beats per minute.

To a Krebs-Henseleit buffer was added a mixture of 8.2 mM [1,6-$^{13}C_2$]glucose, 0.63 mM [U−^{13}C]fatty acids, 0.17 mM [1,3-$^{13}C_2$] acetoacetate, 1 microunit/mL of insulin, and 2% bovine serum albumin to solubilize the fatty acids. Fig. 1 details the ^{13}C labeling patterns generated with this perfusion condition. Fatty acids will generate uniformly labeled acetyl-CoA, ketones will produce C1 labeled acetyl-CoA,

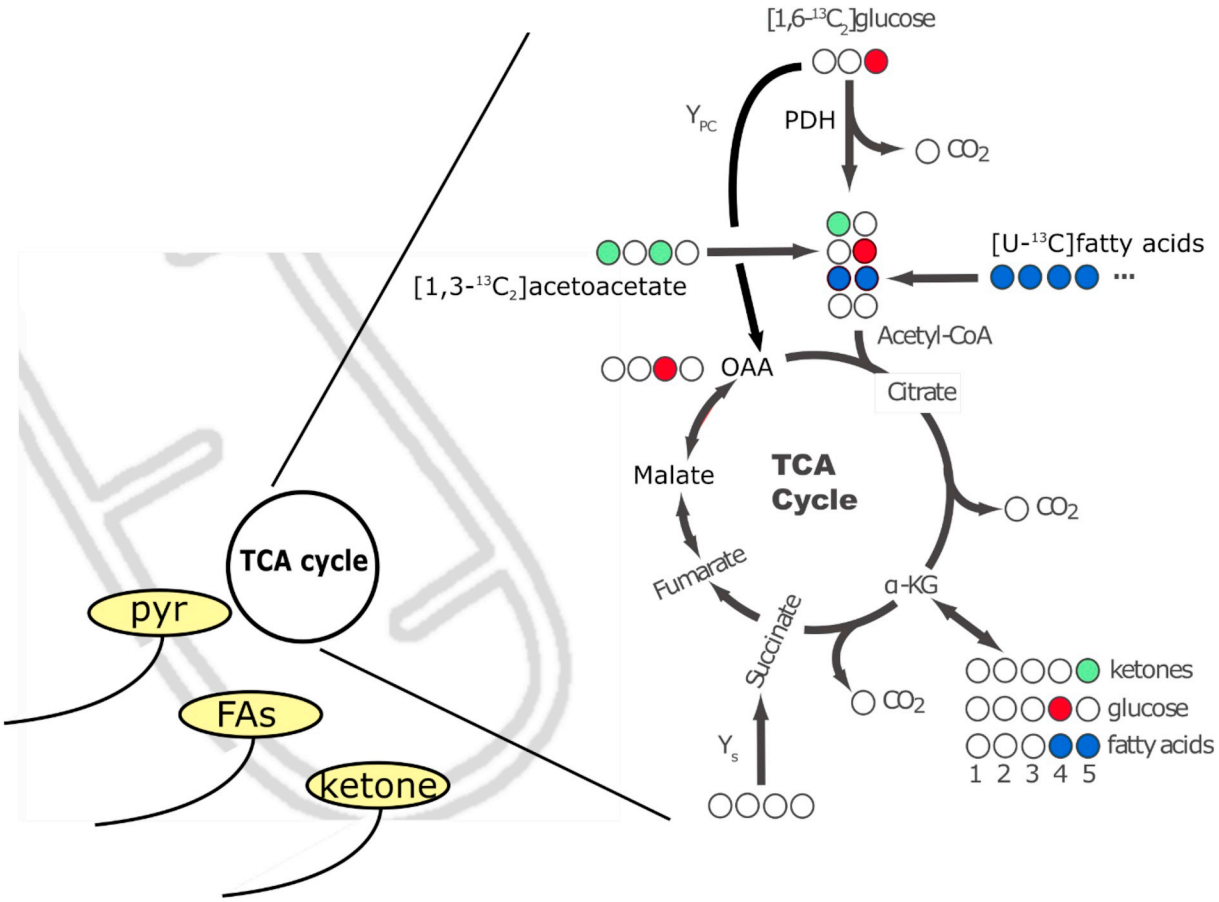

Fig. 1. Substrate delivery to mitochondria and subsequent oxidation. A) Metabolic scheme for the carbon labeling of glutamate that would be expected on the first turn of the TCA cycle upon administration of [1,3-$^{13}C_2$]acetoacetate, which would produce C5-labeled glutamate (light green). Administration of [1,6-$^{13}C_2$]glucose produces methyl-labeled pyruvate, and subsequently C4-labeled glutamate (red). Uniformly ^{13}C enriched fatty acids produce doubly-labeled glutamate on the first turn of the cycle (blue). Because of the J-coupling that exists when ^{13}C nuclei share a chemical bond, and the chemical shift selectivity of the NMR experiment in general, the various isotopomers of glutamate can be readily identified. Alternatively, pyruvate carboxylation by either pyruvate carboxylase or the malic enzyme can act to produce oxaloacetate from pyruvate, which would result in a [2-^{13}C]oxaloacetate (OAA, red). Due to rapid backwards exchange into the symmetric intermediate fumarate, [2-^{13}C]OAA and [3-^{13}C]OAA come to an equal distribution when at steady state. (For interpretation of the references to colour in this figure legend, the reader is referred to the web version of this article.)

and glucose will produce C2 labeled acetyl-CoA. Due to the use of [1,6-$^{13}C_2$]glucose and [1,3-$^{13}C_2$]acetoacetate, their fractional oxidation can be directly obtained from the multiplets associated with glutamate. If only [1-^{13}C]glucose or [1-^{13}C]acetoacetate was used, a normalization for the unlabeled contribution of the C6 of glucose and the C3 of acetoacetate would be necessary. Hearts were freeze-clamped in a pair of aluminum tongs immersed in liquid nitrogen and stored at −80 °C until extraction.

2.4. NMR analysis of tissue extracts

The perchloric acid method was used to isolate water soluble metabolites [33]. The water soluble fraction was analyzed without further purification. The samples were pH corrected, lyophilized, and resuspended in 180 μL of D_2O and placed in a 3 mm NMR tube. NMR samples were run on a 14.1 T Bruker Avance 3 HD console paired with a 10 mm broadband cryoprobe. A 45 degree flip angle was used to collect ^{13}C spectra with 65,536 data points (0.91 s acquisition time) and broadband proton decoupling. The total time to repeat (T_r) was 3 s. A spectral width of 35 kHz was used and sample temperature was controlled at 25° C. Relative peak areas for the ^{13}C spectra were obtained by spectral line-fitting using software from Advanced Chemistry Development Labs (ACD, Toronto, Canada). Proton spectra were collected with the first slice of the Bruker noesypr1d sequence with a 4 acquisition time and a 5 s TR. Water saturation was accomplished using a 1 s continuous wave presaturation pulse and 200 ms of water saturation during the delay between the 2nd and 3rd pulses of the NOESY pulse sequence. Concentrations of eight metabolites were estimated using Chenomx software (Chenomx, Inc., Alberta, Canada) and subsequently normalized to the heart rate. Fractional ^{13}C enrichment of the lactate and alanine in the extracts was measured by line-fitting of the ^{1}H—^{13}C *J*-coupled multiplet in the proton spectra using ACD software.

2.5. Modeling

The carbon-13 NMR spectra of glutamate were analyzed by the method of Sherry, et al. for the assessment of TCA cycle turnover and fractional utilization of available substrates [34]. The relative ratios of the multiplets of C2, C3, C4, and C5 were determined and used as input for the tcaCALC program [34]. In addition, the relative ratio of the total C4 resonance area to that of the C3 was used as an input. The C4/C3 ratio reflects the dilution of carbon-13 labeling at the C3 position of glutamate due to anaplerotic flux. TcaCALC produced estimates of the fractional enrichment of the acetyl-CoA pool as well as the fractional contributions of ketone, fatty acid, glucose, and endogenous substrate oxidation to oxygen consumption. The endogenous contribution of substrate to acetyl-CoA is obtained by subtraction (normalization to 1). In the heart, it is assumed that O_2 consumption is exclusively related to

Table 1
Initial conditions for tcaCALC modeling. Subsequent optimization of the values is accomplished by a Levenberg-Marquardt gradient-descent algorithm. Fractional CHO is the initial estimate of the carbohydrate versus non-carbohydrate sources of acetyl-CoA.

Pathway	ModYPC	ModYS-YPC
Ketone	0.34	0.34
Fatty acid	0.17	0.17
[3-^{13}C]lactate fraction	0.9	0.9
Fractional CHO	0.4	0.4
Y_{PC}	0.1	0.1
Y_s	n/a	0.1

oxidation of NADH and ATP production via oxidative phosphorylation. Measurements of fractional ^{13}C enrichment of alanine was directly incorporated into the constraints used for tcaCALC in some circumstances [35]. A model of oxidative flux that included pyruvate anaplerosis (Mod_{YPC}) was first tested using the estimated starting values seen in Table 1 (see Fig. 1 for pathway identification). A second model that included anaplerosis from either succinyl-CoA or glutamine (Y_s) and pyruvate was also used to fit the isotopomer data ($Mod_{YS\text{-}YPC}$).

2.6. Real-time PCR

RNA was isolated from mouse hearts with the Aurum Total RNA Fatty and Fibrous Tissue Kit (Bio-Rad). Purity and concentration were assessed by NanoDrop. Reverse transcription was performed with 500 ng of RNA and iScript Reverse Transcription Supermix (Biorad) in a thermocycler: 25 °C 5 min, 42 °C 30 min, 85 °C 5 min, 25 °C 5 min. Transcript levels were determined by quantitative PCR using a Roche Lightcycler 480 II using iTaq Universal SYBR Green Supermix (Biorad) with reactions of 95 °C for 5 min, followed by 45 cycles of [95 °C 10s, 56 °C 10s, 72 °C 20s]. The following primer sequences were used for each transcript: Bdh1_mouse_f 5' CTTGGAGAGCCTAGGCAACG, Bdh1_mouse_r 5' TTCTGGTGGCTCCCAAAGC, Oxct1_mouse_f 5' GAGG ACGGCATGTACGCTAA, Oxct1_mouse_r 5' TCCGCATCAGCTTCGTC TTT, Hmgcs2_mouse_f 5' AGCTACTGGGATGGTCGCTA,Hmgcs2_ mouse_r 5' ACGCGTTCTCCATGTGAGTT, Slc16a1_mouse_f 5' ACGCCG GAGTCTTTGGATTT, Slc16a1_mouse_r 5' TGAGGCGGCCTAAAAGTGG. Relative transcript levels were calculated using the comparative Ct method normalized to 18S. From 5 to 7 animals were used for the sham controls, with $N = 5$ for TAC, 1-week, and $N = 3$ for TAC 3-week and sTAC 1-week.

2.7. Echocardiography

Transthoracic echocardiography was performed using a VisualSonics Vevo 2100 system equipped with MS400 transducer (FUJIFILM Visual Sonics Inc., Toronto, Ontario, Canada) in conscious mice. Left ventricular two-dimensional parasternal short axis view was obtained and optimal M-mode scans were recorded at mid ventricular level, as indicated by the presence of papillary muscles, to measure ventricular dimension and wall thickness. All parameters were measured at least 3 times and the averages were presented. Parameters include: end-diastolic interventricular septal wall (IVSd), end-systolic interventricular septal wall (IVSs), left ventricular internal end-diastolic diameter (LVIDd), left ventricular internal end-systolic diameter (LVIDs), left ventricular end-diastolic posterior wall (LVPWd), left ventricular end-systolic posterior wall (LVPWs), heart rate (HR). The percentage of fractional shortening (FS%) was calculated as [(LVIDd − LVIDs)/LVIDd] × 100. Left ventricular (LV) mass was calculated using the M-Mode (cubic) method: LV mass = 1.05[(LVIDd + IVSd + LVPWd)^3 - (LVIDd)^3]. To confirm the success of aortic constriction and estimate the degree of pressure overload, one week after surgery mice were anesthetized with isofluorane 1.0–1.5% and pulsed wave (PW) Doppler measurements of blood flow velocities in the right (RC) and left (LC) carotid arteries were recorded. For sham and sTAC, $N = 5$ animals were used.

2.8. LC/MS metabolomics

Sham and sTAC mice were anesthetized with isoflurane and the heart was immediately excised and frozen in liquid nitrogen to preserve relative metabolite pool sizes. The frozen hearts were ground in a mortar and pestle, then extracted using the chloroform/methanol method. Samples were analyzed ($N = 6$ control, N = 5 sTAC) using a quadrupole LC/MS and a targeted amino-acid/organic acid panel composed of 22 metabolites. A similar panel was used to assess acylcarnitines, producing a total of 66 identified metabolites. Data was log2 scaled (fold change) for display purposes.

2.9. Statistical analysis

The data was analyzed for significant differences using GraphPad Prism (La Jolla, CA) or Microsoft Excel (Redmond, WA). For all calculations the noise was considered to be Gaussian and *t*-tests assumed two tails. For the mRNA expression levels, the sham controls, 1 week and 3 week TAC, and sTAC hearts were compared using one-way ANOVA analysis and Dunnett's multiple comparison tests. A *P*-value < .05 was considered significant. For the ^{13}C and ^{1}H NMR spectra (which compared only the sham and sTAC models), multiple *t*-tests were used with a *P*-value < .05 considered significant. No correction was made for multiple comparisons and data was not assumed to have equal variance. The error bars on all graphs reflect the standard deviation of the measured values. Due to the larger number of metabolites assayed by the LC/MS panels, the peak intensities were normalized to tissue weight, then analyzed by Metaboanalyst. The data was Pareto scaled and log normalized before analysis by t-test using an FDR multiple sample correction at 0.05.

3. Results

3.1. Heart performance and mRNA encoding

To assess metabolic remodeling in the failing heart, mice were put into two groups, sham surgery or sTAC surgery. Dilated cardiac hypertrophy and failure was confirmed by ultrasound measurements (Table S1, sTAC column). As expected, aortic constriction resulted in a significant increase in the heart weight (Fig. 2, a) [28]. Measures of O_2 consumption in the hearts at the time of Langendorff perfusion showed a significant increase in the sTAC model (Fig. 2, b). In separate experiments, levels of mRNA encoding for the proteins β-hydroxybutyrate dehydrogenase (BDH1), 3-oxoacid-CoA transferase 1 (OXCT1), and the monocarboxylate transporters (SLC16A1) were measured using qPCR. To differentiate between changes due to the hypertrophic response and those due to heart failure per-se, expression of these RNAs was also measured in TAC models at 1 week and 3 week time points (Fig. 2, c-e). In our hands, the 1 week TAC time point gives a sample in which the heart is undergoing compensated hypertrophy, while the 3 week TAC and the 1 week sTAC model show signs of decompensated hypertrophy, with thinning of the ventricle wall and decreased systolic function, as well as the increase in lung weight emblematic of heart failure in these models, sTAC being the more severe of the two [28]. The mRNA levels for each gene were significantly different from the sham surgery by one-way ANOVA analysis. Multiple comparisons using the sham surgery as a control found a variety of significant differences for each gene tested. The mRNA associated with BDH1 and SLC16A1 followed similar trends, with an immediate increase at 1 week of TAC and a subsequent decline. For SLC16A1, the decline at 3 weeks of TAC and in sTAC was significantly different from the sham surgery. In contrast, OXCT1 never upregulated, and showed pronounced downregulation at 3 weeks of

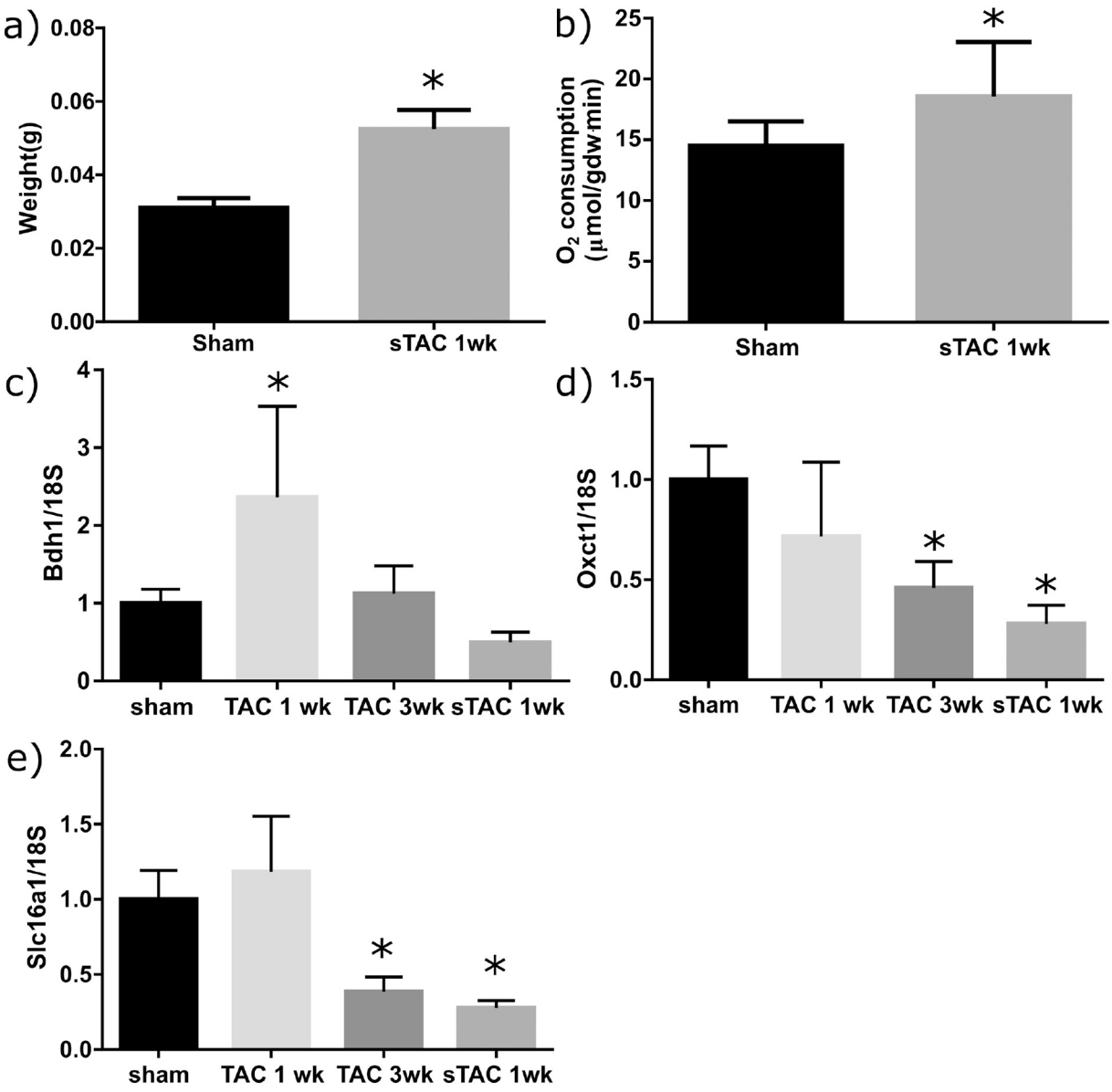

Fig. 2. (a). The sTAC hearts ($N = 7$) were significantly larger in weight compared to the sham controls ($N = 8$). (b) The oxygen consumption for the sTAC hearts was significantly higher even after normalization to the weight of the tissue. (c) Gene expression for BDH1 in hearts ($N = 3$ to 7) after a sham surgery, 1 week and 3 weeks of TAC, and 1 week following the sTAC surgery (model studied with metabolomics and flux analysis here). Asterisks denote significant differences for each column as determined using one-way ANOVA with Dunnett's multiple comparisons test ($P < .05$). (d) Expression levels for Oxct1 across treatment types. (e) Expression levels for Slc16a1. For number of subjects for c-e, see section 2.6.

TAC and in sTAC. These data suggest in our model an increase in BDH1 associated with hypertrophy and a decrease in a number of ketone pathway genes associated with heart failure. With these changes in genetic signature, it was expected that ^{13}C flux analysis would also show significant differences.

3.2. Carbon-13 isotopomer analysis

Carbon-13 NMR of the heart extracts produced spectra with excellent signal-to-noise (SNR) ratio (Fig. 3). Due to the ^{13}C enrichment in each of the available substrates, the resonances for each carbon of glutamate display multiple lines associated with homonuclear J-couplings to adjacent carbon-13 labeled positions. In some instances, long range J-couplings (J = 3.1 Hz) are evident as well, as in the case of the C5 position of glutamate (Fig. 3, inset). While this data can be harvested to provide further information in some circumstances, it was not taken advantage of for the analyses here [36]. The relative areas of the glutamate multiplets as well as the C4/C3 ratio were input into tcaCALC using a model that allowed fractional oxidation from a variety of substrates as well as anaplerosis (Table 1, Fig. 1). The addition of [1,6-$^{13}C_2$]glucose to the perfusate results in ^{13}C labeling at the C3 position of lactate and alanine (Table 2). In both lactate and alanine, the fractional enrichment decreased significantly in the sTAC model, though the absolute change for lactate enrichment was small. In addition, the fractional enrichment of lactate was significantly higher than that of alanine (Table 2). In no case was the ^{13}C enrichment below 80% for either lactate or alanine. Increasing 3-carbon intermediate labeling guided our subsequent model optimization.

TcaCALC analysis for both groups of hearts using Mod_{YPC} (Table 1, Fig. 1) and no constraints on the fractional enrichment of the pyruvate pool produced mediocre fits to the data as assessed by the residual F-values (Fig. S1). In addition, the predicted ^{13}C fractional enrichment of the pyruvate precursor pool was only ~60% for both groups, which is significantly below the measured levels. Using the measured ^{13}C

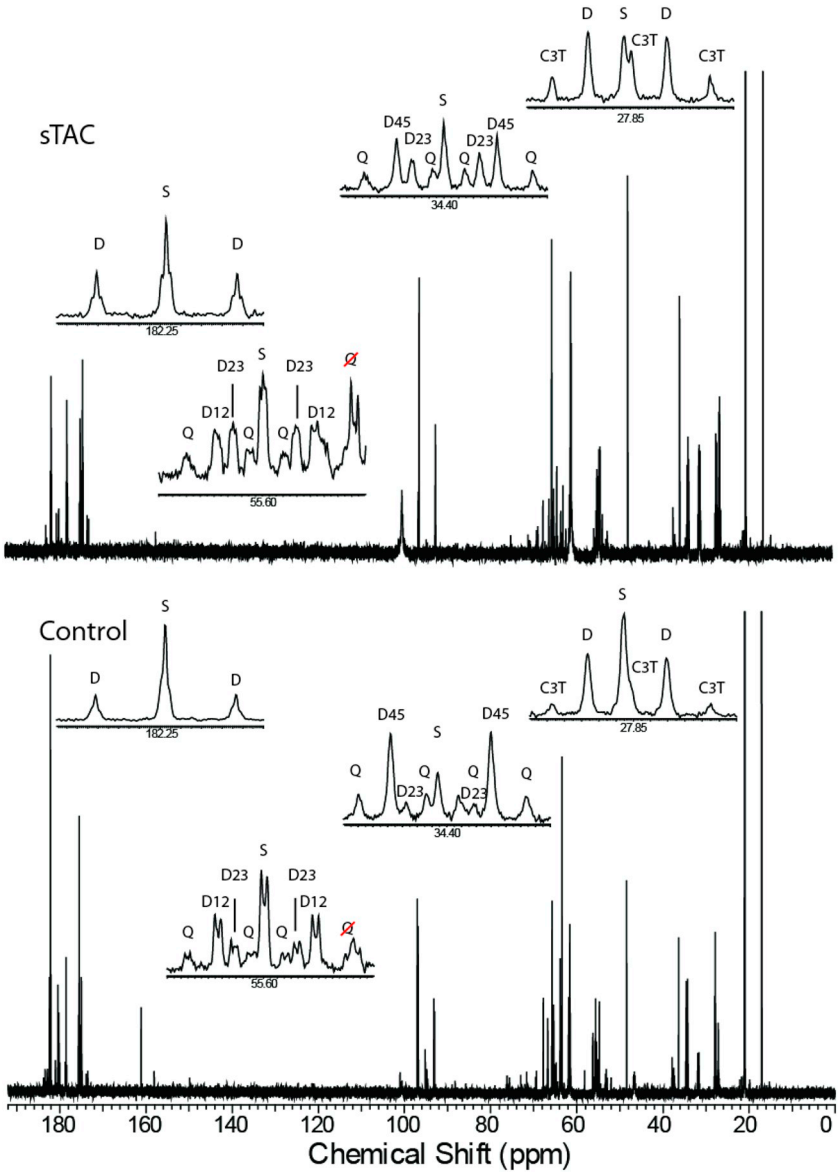

Fig. 3. Carbon-13 spectra with expanded regions obtained for extracts of a heart with a sham surgery (bottom) and with sTAC (top) display the $^{13}C–^{13}C$ j-coupling characteristic of highly ^{13}C-enriched glutamate. The C5 position of glutamate (182.25 ppm) is composed of a singlet (S) and a doublet (D), the ratio of which allows the fractional contributions of ketones to the acetyl-CoA enrichment to be inferred. The C4 position (34.4 ppm) reveals the competition between fatty acids and glucose for the production of acetyl-CoA through the relative ratios of the singlet and D23 doublet to the D45 doublet and the doublet of doublets, or Q, peaks that arise from glutamate enriched at the C3, C4, and C5 positions simultaneously. Glutamate C3 (27.85 ppm) and the C2 (55.6 ppm) provide complementary information. In the case of the C2 position, long range j-coupling to the C5 position reveals the condensation of a ketone moiety with an oxaloacetate enriched in a previous turn of the TCA cycle. The Qs with red strike-throughs denote areas that were approximated by using the average of the other 3 multiplet components not subject to extreme overlap with other resonances.

Table 2
Fractional enrichment of lactate and alanine in sham ($N = 8$) and sTAC hearts ($N = 7$).

	[3-^{13}C]lactate	[3-^{13}C]alanine
Sham	95.4 ± 1.0	88.6 ± 4.7
sTAC	92.8 ± 1.1	81.0 ± 4.3

Table 3
Absolute anaplerosis via pyruvate carboxylation or via succinate or glutamine uptake. The change in Y_s was significant by *t*-test (P value 0.005).

	Y_{PC}	Y_s
Sham	0.05 ± 0.03	0.06 ± 0.05
sTAC	0.03 ± 0.04	0.12 ± 0.02

enrichment of alanine as a constraint for tcaCALC produced worse fits as assessed by the F-values, though apparent differences between the sham and sTAC hearts in PDH flux and pyruvate carboxylation were emphasized (Fig. S1). Given the decreased quality of the fits produced when more prior information was provided, we proposed a more complicated model of myocardial metabolism ($Mod_{YS\text{-}YPC}$, Table 1). Using this model, the residuals decreased in amplitude. In this case, pyruvate carboxylation was not significantly different between groups, but anaplerosis of unlabeled substrates through either succinyl-CoA or glutamate dehydrogenase. As a final check of the suitability of this model, the alanine ^{13}C enrichments were included as a constraint (Table 3). This additional information caused the residuals for both groups to decrease further. Given the superior fits, we chose $Mod_{YS\text{-}YPC}$ as the optimal model of TCA cycle function.

Once this model was chosen, absolute TCA cycle turnover was calculated using the specific efficiency of each supplied substrate (Fig. S2) [14]. Using this method, total TCA cycle turnover was marginally elevated in the sTAC heart, but the contribution of glucose to acetyl-CoA production was significantly increased (Fig. 4). As ketones are less efficient than glucose for NADH production per mol of O_2 consumed, this change explains the non-significant increment in total TCA turnover in the sTAC mice despite a significant increase in O_2 consumption. However, flux through Y_s essentially doubled ($P = .005$) in the sTAC model of heart failure while Y_{PC} was not significantly different (Table 3). Another source of O_2 consumption is the utilization of ATP generated by glycolytic flux. To account for O_2 consumption related to lactate that is not ultimately oxidized in the TCA cycle, lactate in the efferent

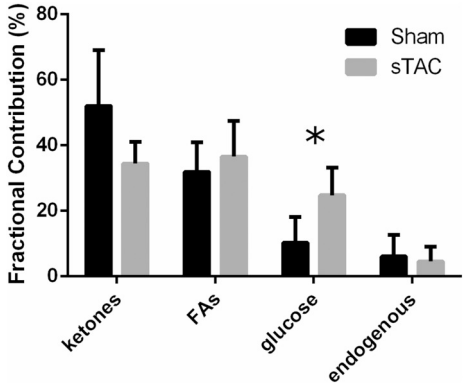

Fig. 4. Fractional contributions of ketones, fatty acids, glucose, and unlabeled endogenous sources to acetyl-CoA production in the perfused mouse heart. Fractional glucose oxidation was significantly greater in the sTAC hearts ($P < .05$).

perfusate was measured by standard assay. After normalization for 2 lactates/glucose molecule, lactate production was measured as 1.89 ± 0.99 μmol/gdw·min in the control hearts and 2.83 ± 1.43 μmol/gdw·min in the sTAC hearts ($P = .18$, NS). While glycolytic flux is high in absolute terms compared to V_{tca}, the relatively low production of NADH at the glyceraldehyde-3-phosphate dehydrogenase reaction means that this mechanism has a passingly small effect on ATP production in both experimental conditions.

3.3. ^{1}H NMR of perfused hearts

^{1}H NMR analysis of the extracts used for the ^{13}C spectroscopy indicated that relative concentrations of lactate and alanine were not significantly between groups (Fig. S3). Glutamine concentration was unchanged, but glutamate concentration was significantly decreased in the sTAC as was the acetone concentration. Succinate could not be reliably detected. Lactate and alanine were unchanged in total concentration.

3.4. LC/MS metabolomics of excised hearts

Mass spectrometry based metabolomic analysis of hearts collected directly from the mice in separate experiments (without perfusion) in general showed trends that agreed with previous work (Figs. S4-S6). However, out of both the acylcarnitine panel (66 identified metabolites) and the organic/amino acids (22 identified metabolites), only α-ketoglutarate showed a significant difference after FDR correction.

4. Discussion

4.1. Mechanical function and mRNA expression in the sTAC model

The sources of energy production as well as the role of ATP availability in heart failure associated with pressure-overload hypertrophy are controversial [17,37]. In many patients, persistent afterload stress leads to hypertrophic heart disease that decompensates to failure. By varying the size of constriction two distinct models of pressure-overload have been developed; one produces stable compensated hypertrophy (TAC), the other progresses to decompensated failure (sTAC) [28]. Animals that undergo sTAC develop hypertrophic growth of the heart and progressive deterioration of LV systolic function as measured by echocardiographic recordings in the current study (Table S1). Lung-to-body-weight ratios also significantly increase in this model [28]. The surgery produced significant changes in heart mass as expected (Fig. 2), with commensurate changes in heart function as assessed by ultrasound (Table S1). The fractional ejection numbers were very high for the control animals. We assign this efficiency to the fact that our protocol for assessing EF in awake animals is built on repeated, daily exposure to the procedure, so that the mice are not stressed during the studies. Note the similarity of comparable values across the control and TAC (Table S1). All of the physiological and mechanical features are similar to the evolution of heart failure during pressure-overload hypertrophy in humans.

To provide greater context for the analysis of the sTAC energetics, mRNA levels for other models are also reported. The analysis of mRNA levels of enzymes essential for oxidative metabolism in the mitochondria produced an interesting picture of its regulation in both the TAC and sTAC models. Previous work in a similar but not identical murine model outlined the role of increased ketone oxidation in the failing heart. That model used a combination of pressure overload hypertrophy with addition of a myocardial infarction to induce heart failure [24]. In that case, BDH1 mRNA levels increased across the spectrum of compensated hypertrophy to outright failure. Similar results were reported in a small cohort, human trial [27]. The results in humans were collected from patients undergoing transplant at dilated failure, but the etiology of the HF was not further discussed [27]. Here, after an initial spike in BDH1 levels at 7 days (TAC), hearts are not significantly different when comparing the controls to the sTAC data (Fig. 2,c). The high pressure caused by the sTAC surgery likely induces different metabolic effects than some other models [18,24]. OXCT1 levels, alternatively referred to as SCOT1 levels, showed a progressive decline across hypertrophy and failure (Fig. 2,d), mirroring other work in a heart failure model [38]. The trend of increased expression of the monocarboxylate transporter (MCT) gene (SLC16A1) at 1 week of TAC and a subsequent decrease with sTAC matches the BDH1 expression (Fig. 2,e). Overall, mRNA levels could not be used to predict an increment in ketone or monocarboxylate (lactate, pyruvate) metabolism. These data are in contrast to what has been observed in the TAC/MI model (24). This may be due to inherent differences in the causes of HF in these two models (infarction vs decompensated hypertrophy). The earlier studies pointed to BDH1 activity as the rate limiting step in ketone utilization by the heart (24). However, this study uses acetoacetate as a tracer, which prevents a ready estimate of BDH1 flux.

4.2. sTAC produces increased fractional glucose utilization

Carbon-13 NMR isotopomer analysis [39–41] is a well validated method that allows the fate of multiple labeled substrates to be measured simultaneously and quantitatively. The triple tracer technique used here allows simultaneous measurement of multiple sources of acetyl-CoA: unlabeled, attributed to endogenous contributions, and ketone, fatty acid, and carbohydrate sources (Fig. 1). This method reduces the number of animals needed for a study, and should also increase the reproducibility and rigor of research, as biological variability across multiple groups needed when using less sophisticated labeling schemes is suppressed. Due to the chemical shift selectivity of the NMR experiment, it is straightforward to assign the fractional oxidation of each of the available substrates, whether it is [U-^{13}C]FAs, [1,3-$^{13}C_2$] acetoacetate, or [1,6-$^{13}C_2$]glucose (Fig. 1). The distribution of carbon-13 isotopomers is modeled to produce estimates of TCA cycle turnover [34]. When indexed against O_2 consumption measurements using the afferent and efferent perfusate, absolute TCA cycle turnover can be inferred using known models of myocardial metabolism [14]. This method assigns an R-value for the efficiency of each substrate for production of a reducing equivalent per mol of O_2 consumed, with glucose having an R-value of 3, mixed fatty acids assigned a value of 2.81, and acetoacetate having a value of 2. In this case, the endogenous (unlabeled) contribution to acetyl-CoA was small. For modeling of absolute flux, the unlabeled component was attributed to endogenous glycogenolysis, and assigned an R-value of 3. The metabolic model included Y_{PC} and Y_s, as well as oxidation of the supplied substrates. Fitting of the NMR data produces estimates of TCA turnover that depend upon the

fractional contribution of each substrate (Fig. S2), but not on the absolute O_2 consumption. In this data set, a significant increase in O_2 consumption (Fig. 2) did not translate to increased TCA cycle flux, as in the sTAC heart the fractional oxidation of glucose was increased. Glucose oxidation is the most efficient of all substrates per mol of O_2 consumed. Therefore, after scaling by the R-values, TCA flux was not significantly different between control and sTAC. Using this analysis allows us to detect the change in Y_s, but also infers significant changes across all substrates in terms of absolute flux. The estimate of Y_s and Y_{PC} does not depend on the O_2 consumption, but only on the NMR spectra. Therefore, changes in anaplerotic fluxes from control to sTAC are robust, and not subject to contention based on the further discussion regarding low work efficiency.

The sTAC heart is in a state of low mechanical work efficiency (Table S1). Increased O_2 consumption in this case is not due to increased oxidative phosphorylation, but rather uncoupling in the mitochondria [7]. Therefore, absolute turnover estimates (Fig. S2) should only be interpreted in the light of the fractional changes that can be inferred (Fig. 4). With this restriction, only glucose oxidation was significantly different, with concomitant changes apparently shared by the ketone and FA contributions not reaching statistical significance. In the current study, BDH1 activity was assumed high, consistent with the use of [β-hydroxybutyrate] / [acetoacetate] as a method to calculate redox state of the mitochondria. Nevertheless, even with the low concentration of acetoacetate used here (0.17 mM), it is possible oxidation of ketones would be different if a mixture including β-hydroxybutyrate was available. Experiments using physiological concentrations of both labeled β-hydroxybutyrate and acetoacetate would be the most effective way of performing the triple-tracer experiment described here, as this method would retain sensitivity to BDH1 flux.

Flux through the Embden-Meyerhof pathway is remarkably active in both the sham surgery and experimental animals, as evidenced by the highly enriched [3-^{13}C]lactate and [3-^{13}C]alanine detected in the heart extracts (Table 2). Previously alanine has been shown to be a superior marker of mitochondrial pyruvate concentration as compared to lactate [35]. For this reason, whenever the pyruvate enrichment was bounded for tcaCALC analysis, the alanine ^{13}C enrichment was used as a surrogate. Alanine fractional enrichment was significantly lower than lactate. Pyruvate is normally very low in concentration, and typically undetectable by NMR. Lactate production as measured in the efferent perfusate was not changed when normalized to heart weight (1.89 ± 0.99 μmol/gdw·min, sham, and 2.83 ± 1.43, sTAC), nor was it different in the extracted tissue (Fig. S3). Fractional enrichment in lactate was significantly decreased in sTAC, but the absolute difference in enrichment was very small. Therefore, the data does not support an increased role for glycolysis in energy production. Other work referenced lactate enrichment to the ^{13}C labeled substrate, in which case the fraction of labeled lactate as a ratio to glucose was seen to increase in HF [18]. This previous observation from the tissue alone indicates that flux through glycolysis was indeed increased in that model, which was produced using an extended TAC (8 week) protocol. We did not measure glucose extraction in the afferent versus efferent perfusate. In experiments here, lack of change in tissue lactate and alanine concentration and a small change in fractional enrichments is more consistent with the observation of increased glucose utilization for acetyl-CoA production. Without the extracted glucose metric, it is not straightforward to compare data here versus that in Kolwicz, et al. [18].

4.3. sTAC increases anaplerosis apart from pyruvate carboxylation

Using a model that included only pyruvate carboxylation as a source of anaplerosis, flux through PDH was elevated in sTAC, but estimates of pyruvate carboxylation seemed extremely high, exceeding flux through PDH. Further examination of the residuals revealed that Mod_{YPC} (Table 1, Fig. S1) failed to produce accurate estimates of the glutamate C4/C3 ratio. Incorrect modeling of this ratio is a tell-tale sign that anaplerosis from unlabeled precursors must be included in the model. Inclusion of Y_s as a functioning pathway as well as the fractional enrichments of alanine resulted in fits with progressively better residuals as well as logical estimates of Y_{PC} and Y_s as a fraction of V_{tca} (Table 3, Fig. S1). Due to these observations, it appears a model of myocardial metabolism that includes both pyruvate carboxylation and anaplerosis through succinyl-CoA or via α-ketoglutarate is the minimally sufficient model. The NMR experiment does not identify the mechanism of pyruvate carboxylation, be it through pyruvate carboxylase or the malic enzyme, though previous work indicates the malic enzyme is more active in the heart [42]. Here, pyruvate anaplerosis is denoted as pyruvate carboxylation, without assumption about the enzymatic mechanism(s).

Using the $Mod_{Ys\text{-}YPC}$ model, Y_{PC} in the failing heart is unchanged, as is the oxidation of endogenous, unlabeled substrates. This is an indication that glycogenolysis in the failing heart is not significantly different from the sham animals. Presumably, if glycogenolysis is increased, it could also serve to produce unlabeled pyruvate for production of lactate or for anaplerotic flux through Y_{PC}. However, as discussed earlier, Mod_{YPC} with unconstrained 3-carbon precursor enrichment produced worse fits than $Mod_{Ys\text{-}YPC}$. Y_s as a fraction of V_{tca} is significantly increased in the sTAC hearts. Another possible source of unlabeled acetyl-CoA is acetate that is naturally occurring in albumin solutions [43]. Without further experiments, the fractional oxidation of acetate associated with the albumin versus unlabeled products of glycogenolysis remains undetermined. Since the fraction of unlabeled acetyl-CoA is the same across the control and sTAC models, this factor was deemed insignificant.

Previous work used the concentration of succinate as a biomarker of increased ketone utilization via SCOT mediated utilization of β-hydroxybutyrate [24]. Here succinate trended lower without reaching a statistically different decline in the failing heart (Fig. S4). This is consistent with the similar non-significant decrease in fractional ketone oxidation observed in the parallel perfused heart experiments (Fig. 4). It's not clear where the differences arise between the sTAC model and the one previously reported; it may be the type of damage (ischemia vs pressure-overload induced failure) or it may be mouse sex (female in their study vs male in ours) or strain differences. Regardless, the data suggests that a one-size-fits-all model for metabolic changes in heart failure is unlikely. Heart failure is a clinical syndrome, not a disease, and as such is triggered by a variety of stressors and other concomitant pathophysiologies. The data here suggest that pyruvate anaplerosis is not necessarily upregulated in late stage of pressure overload induced HF, as compared to hypertrophy [15]. The results presented are a first step for further analysis of the sTAC model, as it relates only estimates of substrate selection, not ATP production via ^{31}P NMR.

5. Conclusion

Due to the chemical selectivity of ^{13}C NMR, oxidative metabolism can be assessed using a perfusate that contains three different labeled precursors that are nutrients used for acetyl-CoA production. The data shows a significant increase in the fractional production of acetyl-CoA from glucose, and anaplerotic flux from sources other than pyruvate is necessary to produce a model making the most accurate fits of the NMR data. The significant increase in Y_s flux paired with the decrease in TCA cycle intermediate pool sizes corroborates previous hypotheses related to increased protein turnover in the failing heart [44]. As protein turnover increases, it is expected that cataplerosis of the TCA cycle intermediates used in amino acid biosynthesis will increase. With this depletion of intermediates, it follows that anaplerosis from some source must increase for mass balance purposes and the proper function of the TCA cycle. The source of anaplerotic substrate was not identified, and exogenous glutamine was not supplied in the perfusate [30]. Future experiments will test whether increased anaplerosis is via succinyl-CoA or glutamine. Branched chain amino acids (BCAA) could possibly be

catabolized, but previous work showed that BCAA catabolic genes were downregulated in a similar model [45]. Modulation of anaplerosis is a well-known theme in the pathophysiology of tissue remodeling [46]. Heptanoate was not found to provide significant beneficial effects in extracorporeal membrane oxygenation [47]. However, the findings of depleted TCA intermediates in HF is one of the few points that the literature agrees upon. The observation of increased Y_s in this model emphasizes again the need for a deeper understanding of anaplerosis in the context of HF.

5.1. Future directions

Ideally, these experiments would be performed in working mode, as opposed to Langendorff, which provides no back pressure. The effects of work are known to modulate substrate selection, increasing FA consumption with increasing load [48]. While the fraction of glucose contributing to acetyl-CoA production was elevated here, an increasing fraction of FA oxidation could prevent a concomitant increase in glucose oxidation. Confirmation of increased relative glucose oxidation in the working model would be welcome.

Funding sources

CM was supported by NIH grant P41-EB015908. MM was supported by NIH -DK105346, HD087306, DK112865, P41122698, U24DK097209, R37-HL034557, and NSF DMR 1644779. The sponsors did not contribute to the study design. AT, FA, GS, and TG were supported by NIH-HL120732, HL126012, and HL128215. AT, FA, GS, and TG were also supported by American Heart Association grants 14SFRN20510023 and 14SFRN20670003.

Declaration of Competing Interest

None.

Acknowledgements

MEM would like to thank Dr. Shawn Burgess for many helpful discussions regarding intermediary metabolism.

Appendix A. Supplementary data

Supplementary data to this article can be found online at https://doi.org/10.1016/j.yjmcc.2019.07.007.

References

[1] A.H. Association, Latest Statistics Show Heart Failure on the Rise; Cardiovascular Diseases Remain Leading Killer, http://newsroom.heart.org/news/latest-statistics-show-heart-failure-on-the-rise;-cardiovascular-diseases-remain-leading-killer>, (2017).
[2] H. Bugger, E.D. Abel, Molecular mechanisms of diabetic cardiomyopathy, Diabetologia 57 (4) (2014) 660–671.
[3] G. Herrmann, G.M. Decherd, The chemical nature of heart failure, Ann. Intern. Med. 12 (8) (1939) 1233–1244.
[4] P.B. Garlick, G.K. Radda, P.J. Seeley, B. Chance, Phosphorus NMR studies on perfused heart, Biochem. Biophys. Res. Commun. 74 (3) (1977) 1256–1262.
[5] P.M. Matthews, J.L. Bland, D.G. Gadian, G.K. Radda, A 31P-NMR saturation transfer study of the regulation of creatine kinase in the rat heart, Biochim. Biophys. Acta (BBA) - Mol. Cell Res. 721 (3) (1982) 312–320.
[6] P.A. Bottomley, MR spectroscopy of the human heart: the status and the challenges, Radiology 191 (3) (1994) 593–612.
[7] S. Neubauer, The failing heart–an engine out of fuel, N. Engl. J. Med. 356 (2007) 1140–1151.
[8] W.C. Stanley, F.A. Recchia, G.D. Lopaschuk, Myocardial substrate metabolism in the normal and failing heart, Physiol. Rev. 85 (3) (2005) 1093–1129.
[9] N. Sambandam, G.D. Lopaschuk, R.W. Brownsey, M.F. Allard, Energy metabolism in the hypertrophied heart, Heart Fail. Rev. 7 (2) (2002) 161–173.
[10] C. Depre, J.-L.J. Vanoverschelde, H. Taegtmeyer, Glucose for the heart, Circulation 99 (4) (1999) 578–588.
[11] M.F. Allard, B.O. Schonekess, S.L. Henning, D.R. English, G.D. Lopaschuk, Contribution of oxidative metabolism and glycolysis to ATP production in hypertrophied hearts, Am. J. Physiol. Heart Circ. Physiol. 267 (2) (1994) H742–H750.
[12] M.E. Christe, R.L. Rodgers, Altered glucose and fatty acid oxidation in hearts of the spontaneously hypertensive rat, J. Mol. Cell. Cardiol. 26 (10) (1994) 1371–1375.
[13] P. Razeghi, M.E. Young, J.L. Alcorn, C.S. Moravec, O.H. Frazier, H. Taegtmeyer, Metabolic gene expression in fetal and failing human heart, Circulation 104 (24) (2001) 2923–2931.
[14] C.R. Malloy, J.G. Jones, F.M. Jeffrey, M.E. Jessen, A.D. Sherry, Contribution of various substrates to total citric acid cycle flux and anaplerosis as determined by 13C isotopomer analysis and O2 consumption in the heart, MAGMA 4 (1) (1996) 35–46.
[15] N. Sorokina, J.M. O'Donnell, R.D. McKinney, K.M. Pound, G. Woldegiorgis, K.F. LaNoue, K. Ballal, H. Taegtmeyer, P.M. Buttrick, E.D. Lewandowski, Recruitment of compensatory pathways to sustain oxidative flux with reduced carnitine palmitoyltransferase I activity characterizes inefficiency in energy metabolism in hypertrophied hearts, Circulation 115 (15) (2007) 2033–2041.
[16] T. Doenst, T.D. Nguyen, E.D. Abel, Cardiac metabolism in heart failure: implications beyond ATP production, Circ. Res. 113 (6) (2013) 709–724.
[17] H. Taegtmeyer, C. Beauloye, R. Harmancey, L. Hue, Insulin Resistance Protects the Heart from Fuel Overload in Dysregulated Metabolic States, (2013).
[18] S.C. Kolwicz, D.P. Olson, L.C. Marney, L. Garcia-Menendez, R.E. Synovec, R. Tian, Cardiac-specific deletion of acetyl CoA carboxylase 2 prevents metabolic remodeling during pressure-overload hypertrophy, Circ. Res. 111 (6) (2012) 728–738.
[19] A.M. Feldman, E.O. Weinberg, P.E. Ray, B.H. Lorell, Selective changes in cardiac gene expression during compensated hypertrophy and the transition to cardiac decompensation in rats with chronic aortic banding, Circ. Res. 73 (1) (1993) 184–192.
[20] H.A. Rockman, R.S. Ross, A.N. Harris, K.U. Knowlton, M.E. Steinhelper, L.J. Field, J. Ross, K.R. Chien, Segregation of atrial-specific and inducible expression of an atrial natriuretic factor transgene in an in vivo murine model of cardiac hypertrophy, Proc. Natl. Acad. Sci. 88 (18) (1991) 8277–8281.
[21] E.O. Weinberg, F.J. Schoen, D. George, Y. Kagaya, P.S. Douglas, S.E. Litwin, H. Schunkert, C.R. Benedict, B.H. Lorell, Angiotensin-converting enzyme inhibition prolongs survival and modifies the transition to heart failure in rats with pressure overload hypertrophy due to ascending aortic stenosis, Circulation 90 (3) (1994) 1410–1422.
[22] C. Riehle, A.R. Wende, V.G. Zaha, K.M. Pires, B. Wayment, C. Olsen, H. Bugger, J. Buchanan, X. Wang, A.B. Moreira, PGC-1β deficiency accelerates the transition to heart failure in pressure overload hypertrophy, Circ. Res. 109 (7) (2011) 783–793 CIRCRESAHA. 111.243964.
[23] P. Zhabyeyev, M. Gandhi, J. Mori, R. Basu, Z. Kassiri, A. Clanachan, G.D. Lopaschuk, G.Y. Oudit, Pressure-overload-induced heart failure induces a selective reduction in glucose oxidation at physiological afterload, Cardiovasc. Res. 97 (4) (2012) 676–685.
[24] G. Aubert, O.J. Martin, J.L. Horton, L. Lai, R.B. Vega, T.C. Leone, T. Koves, S.J. Gardell, M. Krüger, C.L. Hoppel, The failing heart relies on ketone bodies as a fuel, Circulation 133 (8) (2016) 698–705 CIRCULATIONAHA. 115.017355.
[25] K.L. Ho, L. Zhang, C. Wagg, R.A. Batran, K. Gopal, J. Levasseur, T. Leone, J.R. Dyck, J.R. Ussher, D.M. Muoio, Increased ketone body oxidation provides additional energy for the failing heart without improving cardiac efficiency, Cardiovasc. Res. (2019), https://doi.org/10.1093/cvr/cvz045 cvz045.
[26] J.L. Horton, M.T. Davidson, C. Kurishima, R.B. Vega, J.C. Powers, T.R. Matsuura, C. Petucci, E.D. Lewandowski, P.A. Crawford, D.M. Muoio, F.A. Recchia, D.P. Kelly, The failing heart utilizes 3-hydroxybutyrate as a metabolic stress defense, JCI Insight 4 (4) (2019).
[27] K.C. Bedi, N.W. Snyder, J. Brandimarto, M. Aziz, C. Mesaros, A. Worth, L. Wang, A. Javaheri, I.A. Blair, K. Margulies, J.E. Rame, Evidence for Intramyocardial disruption of lipid metabolism and increased myocardial ketone utilization in advanced human heart failure, Circulation 133 (8) (2016) 706–716.
[28] B.A. Rothermel, K. Berenji, P. Tannous, W. Kutschke, A. Dey, B. Nolan, K.D. Yoo, E. Demetroulis, M. Gimbel, B. Cabuay, M. Karimi, J.A. Hill, Differential activation of stress-response signaling in load-induced cardiac hypertrophy and failure, Physiol. Genomics 23 (1) (2005) 18–27.
[29] L. Zhang, J.S. Jaswal, J.R. Ussher, S. Sankaralingam, C. Wagg, M. Zaugg, G.D. Lopaschuk, Cardiac insulin resistance and decreased mitochondrial energy production precede the development of systolic heart failure following pressure overload hypertrophy, Circ. Heart Fail. 6 (5) (2013) 1039–1048.
[30] B. Lauzier, F. Vaillant, C. Merlen, R. Gélinas, B. Bouchard, M.-E. Rivard, F. Labarthe, V.W. Dolinsky, J.R. Dyck, B.G. Allen, Metabolic effects of glutamine on the heart: anaplerosis versus the hexosamine biosynthetic pathway, J. Mol. Cell. Cardiol. 55 (2013) 92–100.
[31] R.R. Russell 3rd, H. Taegtmeyer, Pyruvate carboxylation prevents the decline in contractile function of rat hearts oxidizing acetoacetate, Am. J. Phys. 261 (6 Pt 2) (1991) H1756–H1762.
[32] K.A. Stowe, S.C. Burgess, M. Merritt, A.D. Sherry, C.R. Malloy, Storage and oxidation of long-chain fatty acids in the C57/BL6 mouse heart as measured by NMR spectroscopy, FEBS Lett. 580 (17) (2006) 4282–4287.
[33] K.X. Moreno, S.M. Sabelhaus, M.E. Merritt, A.D. Sherry, C.R. Malloy, Competition of pyruvate with physiological substrates for oxidation by the heart: implications for studies with hyperpolarized [1-13C]pyruvate, Am. J. Physiol. Heart Circ. Physiol. 298 (5) (2010) H1556–H1564.
[34] A.D. Sherry, F.M. Jeffrey, C.R. Malloy, Analytical solutions for (13)C isotopomer analysis of complex metabolic conditions: substrate oxidation, multiple pyruvate cycles, and gluconeogenesis, Metab. Eng. 6 (1) (2004) 12–24.
[35] K.J. Peuhkurinen, J.K. Hiltunen, I.E. Hassinen, Metabolic compartmentation of

pyruvate in the isolated perfused rat heart, Biochem. J. 210 (1) (1983) 193–198.
[36] R.A. Carvalho, E.E. Babcock, F.M. Jeffrey, A.D. Sherry, C.R. Malloy, Multiple bond 13C-13C spin-spin coupling provides complementary information in a 13C NMR isotopomer analysis of glutamate, Magn. Reson. Med. 42 (1) (1999) 197–200.
[37] S. Neubauer, The failing heart–an engine out of fuel, N. Engl. J. Med. 356 (2007) 1140–1151.
[38] R.C. Schugar, A.R. Moll, D. André d'Avignon, C.J. Weinheimer, A. Kovacs, P.A. Crawford, Cardiomyocyte-specific deficiency of ketone body metabolism promotes accelerated pathological remodeling, Mol. Metabol. 3 (7) (2014) 754–769.
[39] F.M. Jeffrey, V. Diczku, A.D. Sherry, C.R. Malloy, Substrate selection in the isolated working rat heart: effects of reperfusion, afterload, and concentration, Basic Res. Cardiol. 90 (5) (1995) 388–396.
[40] F.M. Jeffrey, C.J. Storey, A.D. Sherry, C.R. Malloy, 13C isotopomer model for estimation of anaplerotic substrate oxidation via acetyl-CoA, Am. J. Physiol. Endocrinol. Metab. 271 (4) (1996) E788–E799.
[41] F.M.H. Jeffrey, C.R. Malloy, Respiratory control and substrate effects in the working rat heart, Biochem. J. 287 (1992) 117–123.
[42] R.R. Russell 3rd, H. Taegtmeyer, Changes in citric acid cycle flux and anaplerosis antedate the functional decline in isolated rat hearts utilizing acetoacetate, J. Clin. Invest. 87 (2) (1991) 384–390.
[43] J.J. Kamphorst, M.K. Chung, J. Fan, J.D. Rabinowitz, Quantitative analysis of acetyl-CoA production in hypoxic cancer cells reveals substantial contribution from acetate, Cancer Metabol. 2 (1) (2014) 23.
[44] D. Cao, T. Gillette, J. Hill, Cardiomyocyte autophagy: Remodeling, repairing, and reconstructing the heart, Curr. Sci. Inc 11 (6) (2009) 406–411.
[45] H. Sun, K.C. Olson, C. Gao, D.A. Prosdocimo, M. Zhou, Z. Wang, D. Jeyaraj, J.-Y. Youn, S. Ren, Y. Liu, Catabolic defect of branched-chain amino acids promotes heart failure, Circulation 133 (21) (2016) 2038–2049.
[46] H. Brunengraber, C.R. Roe, Anaplerotic molecules: current and future, J. Inherit. Metab. Dis. 29 (2–3) (2006) 327–331.
[47] M. Kajimoto, D.R. Ledee, A.K. Olson, N.G. Isern, C.D. Rosiers, M.A. Portman, Differential effects of octanoate and heptanoate on myocardial metabolism during extracorporeal membrane oxygenation in an infant swine model, Am. J. Phys. Heart Circ. Phys. 309 (7) (2015) H1157–H1165.
[48] J.R. Neely, M.J. Rovetto, J.F. Oram, Myocardial utilization of carbohydrate and lipids, Prog. Cardiovasc. Dis. 15 (3) (1972) 289–329.